Communications to the Editor

Onset of Chain Entanglements in Block Copolymer Lamellae

Xiaohong Pan[†] and J. Scott Shaffer*[,†,‡]

Department of Chemical Engineering and Department of Materials Science, University of Southern California, Los Angeles, California 90089-1211

Received December 26, 1995
Revised Manuscript Received April 8, 1996

Diblock copolymers, formed by chemically linking two different homopolymer species, provide unique opportunities to study the effects of constraints in polymeric materials. While a blend of two incompatible homopolymers will undergo macroscopic phase separation, the corresponding diblock copolymer is restricted to segregation on mesoscopic length scales. The result is a fascinating variety of diblock copolymer microphases.[1] An additional constraint arises from the microphase formation itself: The junction points between A and B blocks are constrained to lie near interfaces between A-rich and B-rich domains. This localization constraint leads to structural anisotropy as chains stretch away from the A/B interface.[2,3] Dynamical anisotropy is also present, in unequal diffusion coefficients for motion parallel and perpendicular to the lamellae.[4−6]

In this paper, we examine the consequences of localization and anisotropy for another constraint common to all polymeric materials, namely the topological restrictions that prohibit chain crossing and lead to chain entanglements.[7,8] Through a series of computer simulations, we specifically address the following question: Does the formation of the lamellar phase alter the critical molecular weight for the onset of entanglements? This critical molecular weight, M_c, is a fundamental quantity in polymer dynamics, because it delineates two molecular weight regimes, "unentangled" and "entangled", with qualitatively different chain dynamics and transport properties.[9] The effects of microphase formation on the value of M_c are therefore of great importance in molecular theories for the transport coefficients and rheological functions of diblock copolymers.[10−13]

Previous simulations of symmetric diblock copolymers have focused on the nature of the order−disorder transition,[14−16] chain structure in selective solvents,[17] and dynamic properties at a single chain length.[18,19] Here we report simulations that are the first, to our knowledge, to extract diffusion coefficients for symmetric diblocks in the lamellar phase for a range of chain lengths that is wide enough to span the crossover from unentangled to entangled regimes. We can therefore directly identify the critical chain length for the onset of entanglements, N_c, in the lamellar phase and compare it to the value in a bulk, disordered phase.

Our computer simulations employ a kinetic Monte Carlo model of chains on a cubic lattice.[20,21] The general features of the model were inspired by the bond-fluctuation models,[22,23] while the structural characteristics specific to block copolymers were adapted from previous work of Larson.[16] In the absence of monomer−monomer interactions, the present simulations are identical to the simulations of noncrossing homopolymer chains described in refs 20 and 21. Noncrossability is enforced through a special characteristic of the lattice model. By virtue of the lattice geometry, the midpoints of all bonds must lie on a secondary cubic lattice with lattice constant half of that of the main lattice (on which the monomers reside). When attempted moves of monomers are restricted to nearest-neighbor sites, as they are in our kinetic Monte Carlo scheme, any chain crossing in this model must occur through the overlap of bond midpoints.[20] Chain crossings can therefore be rigorously forbidden by tracking the bond midpoints on the secondary lattice and forbidding their overlap. Enforcing this additional constraint on the bond midpoints produces the physically correct, noncrossing chain topology.

Monomer−monomer interactions are introduced and quantified through the energy parameters ϵ_{ij} for contacts between monomers of types i and j. Two monomers are defined to be in contact if the distance between them is $\sqrt{3}$ or less; thus a monomer at a given lattice site has $z = 26$ potential energetic contacts. The interaction energy between like species is taken to be zero; the remaining parameter ϵ_{AB}/kT then controls the incompatibility between the unlike species. Monte Carlo moves satisfying the excluded volume, connectivity, and chain crossing constraints are accepted probabilistically according to the standard Metropolis criterion.[24] Following Larson,[16] an effective interaction parameter χ_{eff} can be defined as follows:

$$\chi_{eff} = \rho z_{eff} \epsilon_{AB}/kT \tag{1}$$

where $\rho = {}^1/_2$ is the overall monomer concentration (the fraction of occupied lattice sites) and z_{eff} is an effective coordination number for the monomer−monomer interactions. As in ref 16, we take $z_{eff} \approx z - 4 = 22$ because there are on average about four intrachain contacts per monomer; in the context of the Flory lattice theory, these should not contribute to the interaction parameter. Including the factor ρ in eq 1 accounts for the reduction in χ_{eff} from the incomplete lattice filling. (There are no energetics ascribed to monomer−vacancy interactions.) The pertinent simulation conditions are summarized in Table 1. The thermodynamic condition used in our simulations, $\chi N \approx 45$, is well into the lamellar region of the phase diagram.

In order to interpret the chain dynamics, we must first characterize the structural properties of the lamellar phases that are formed. Of primary concern are the degree to which junction points are localized and the extent of chain stretching. As in the work of Larson,[16] the lamellar thickness d is roughly proportional to the unperturbed radius of gyration, $R_{g,0}$, characteristic of the weak segregation limit.[1,25,26] The degree of segrega-

[†] Department of Chemical Engineering.
[‡] Department of Materials Science.

S0024-9297(95)01907-3 CCC: $12.00

Table 1. Simulation Parameters[a]

N	N_P	L	ϵ_{AB}/kT	$\chi_{eff}N$
20	492	27	0.200	44
32	381	29	0.130	46
40	491	34	0.100	44
50	593	39	0.080	44
80	570	45	0.056	49

[a] N is the number of monomers per chain; N_P is the number of chains in the simulation cell; L is the edge length of the primary lattice that forms the cubic periodic simulation cell; ϵ_{AB}/kT is the interaction energy for A−B monomer contacts in units of the thermal energy; $\chi_{eff}N$ is the product of the effective Flory−Huggins parameter and the chain length. The lamellar period is given by $L/2$. In all cases, the total fraction of occupied lattice sites, ρ, is $^1/_2$.

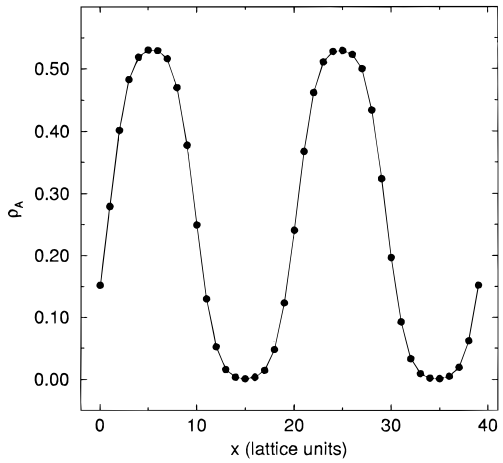

Figure 1. Density profile $\rho_A(x)$ for monomers of type A in the direction perpendicular to the lamellar planes for chains of length $N = 50$. Vacancies show a small preference for the A/B interfaces, so the total segment density rises slightly above $^1/_2$, where $\rho_A(x)$ reaches a maximum.

tion can also be quantified through the monomer density profiles. Figure 1 shows the density profile $\rho_A(x)$ for monomers of type A for chains of length $N = 50$. The lamellae are oriented normal to the x-axis, yielding large-amplitude oscillatory density profiles in this direction. Although the A monomers are completely excluded from the middle of the B-rich lamellae, the interfacial width is a significant fraction of the total lamellar period. In comparison with recent self-consistent field (SCF) calculations of Matsen and Bates,[27] the density profile obtained in our simulations most closely resembles the theoretical profile for the intermediate segregation regime, $\chi N = 25$, in ref 27. The differences between the density profiles of present work and those of the SCF theory may be due to the fairly short chain lengths used in the simulations or the presence of vacancies in the lattice. The vacancies do not distribute themselves uniformly throughout the lamellar structure, for example, but rather they tend to concentrate somewhat near the A/B interfaces. As a result, the maximum density of A segments in Figure 1 is 0.53, higher than the overall average density of 0.5. The vacancies also allow for local density fluctuations. The SCF theory, in contrast, assumes incompressibility and absolutely uniform total density.

To quantify the degree of chain stretching, Table 2 lists the radius of gyration components parallel and perpendicular to the lamellae, $\langle R^2_{g,||}\rangle$ and $\langle R^2_{g,\perp}\rangle$, and the ratio $r = 2\langle R^2_{g,\perp}\rangle/\langle R^2_{g,||}\rangle$. In an isotropic medium, the ratio r is unity; the values of $r \approx 2$ in the lamellar phase with $\chi N \approx 45$ indicate that the copolymer chains are

Table 2. Radius of Gyration Components Parallel and Perpendicular to the Lamellae, $\langle R^2_{g,||}\rangle$ and $\langle R^2_{g,\perp}\rangle$, and the Ratio $r = 2\langle R^2_{g,\perp}\rangle/\langle R^2_{g,||}\rangle$[a]

N	$\langle R^2_{g,||}\rangle$	$\langle R^2_{g,\perp}\rangle$	r
20	4.63	5.39	2.33
32	7.86	7.32	1.86
40	9.80	9.25	1.89
50	12.33	11.88	1.93
80	20.52	17.64	1.72

[a] The unit of length is the lattice constant.

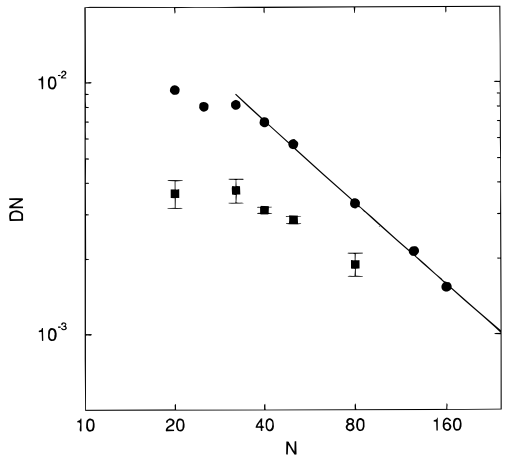

Figure 2. Double-logarithmic plot of the diffusion coefficients, as the product DN, versus chain length for bulk homopolymers (circles), representing the high-temperature disordered copolymer melt with $\chi = 0$, and the lamellar phase (squares) with $xN \approx 45$. In the lamellar phase, the diffusion coefficients reflect motion parallel to the lamellar planes. The solid line indicates the scaling $D \sim N^{-2.09}$.

elongated somewhat in the direction perpendicular to the A/B interface. The degree of chain stretching is far less, however, than in the strong segregation limit or in a strongly stretched polymer brush.[2,28] Taken together, the data in Figure 1 and Table 2 indicate that the lamellar phases formed in the present simulations should be classified in the intermediate segregation regime.

We have set out to determine whether the thermodynamic constraints leading to localization and anisotropy alter the critical chain length for the onset of chain entanglements. The presence of entanglements can be monitored through their effects on the chain diffusion coefficients, $D_{||}$ and $D_\perp$, for motion parallel and perpendicular to the lamellae. Although $D_{||}$ and $D_\perp$ can be comparable near the ODT,[5] the ratio $D_\perp/D_{||}$ decreases with increasing values of χN.[8] For the thermodynamic condition employed here, $\chi N \approx 45$, the penalties for excursions of segments of type A into the B-rich domains (and vice versa) retard diffusive motion in the direction perpendicular to the lamellae.[29] As a result, we do not observe diffusion perpendicular to the lamellae on the time scales of our simulations. (From the mean square displacements, we can estimate that $D_\perp$ is at least an order of magnitude smaller than $D_{||}$.) Instead we focus on the behavior of $D_{||}$; this quantity characterizes the chain mobility within individual layers in the lamellar phase. The diffusion coefficient is calculated from mean square displacement of the center of mass, $\langle \Delta r^2_{cm,||}(t)\rangle = 4D_{||}t$; only data falling in the region $1 \le \langle \Delta r^2_{cm,||}\rangle/\langle R^2_{g,||}\rangle \le 2$ are used to obtain the diffusion coefficient.

Figure 2 contains the main results of the present report. There we show the variation of the diffusion

coefficient, as the product DN, with chain length for the lamellar phase and the homogeneous disordered phase.[30] According to the Rouse theory[9] of unentangled chains in the melt, $D \sim N^{-1}$, so the product DN should be independent of N. Entanglements retard chain diffusion,[9] resulting in diffusion coefficients that are lower than those predicted by the Rouse theory. The onset of chain entanglements can therefore be associated with the critical chain length N_c where the quantity DN begins to decrease with N.[31]

Referring to Figure 2, first note that both the lamellar and disordered phases clearly show a crossover from unentangled to entangled chain dynamics: DN is independent of N for short chains but is a decreasing function of N for long chains. Furthermore, the critical chain length is identical for the two phases; within the resolution of the simulation data, the crossover occurs at $N_c = 30 \pm 5$ for both lamellar and disordered systems. Our main conclusion is therefore that lamellar ordering in symmetric diblock copolymers does not affect the onset of chain entanglements at the thermodynamic condition $\chi N \approx 45$.

Although our simulations indicate that N_c is not affected by the formation of lamellae, this result might be surprising since two characteristics of the lamellar phase could alter the value of N_c. First, chains adopt configurations which are stretched and distorted relative to the bulk phase;[3] the structural features that give rise to entanglements in the bulk[32−34] might be perturbed as a result. Second, the thermodynamic factors leading to the interfacial localization of junction points impose penalties for the excursion of segments of one type into the domain rich in the other. This additional constraint affects the nature of entangled chain dynamics,[8] and it might conceivably shift the chain length at which the constraints of the noncrossing chain topology become significant.[35] These factors may indeed be important for more strongly segregated lamellar phases, with $\chi N \geq 100$ for example. Future efforts will be directed toward simulations in this region of the phase diagram.

Acknowledgment. Financial support from Sun Microsystems, the S. C. Johnson Wax Co., and the James H. Zumberge Research and Innovation Fund (University of Southern California) is gratefully acknowledged. We thank A. Liu, M. Muthukumar, and P. A. Pincus for helpful discussions.

References and Notes

(1) Bates, F. S.; Fredrickson, G. H. *Annu. Rev. Phys. Chem.* **1990**, *41*, 525.
(2) Milner, S. T. *Science* **1991**, *251*, 905.
(3) Halperin, A.; Tirrell, M.; Lodge, T. P. *Adv. Polym. Sci.* **1991**, *100*, 31.
(4) Shull, K. R.; Kramer, E. J.; Bates, F. S.; Rosedale, J. H. *Macromolecules* **1991**, *24*, 1383.
(5) Dalvi, M. C.; Lodge, T. P. *Macromolecules* **1993**, *26*, 859.
(6) Ehlich, D.; Takenaka, M.; Okamoto, S.; Hashimoto, T. *Macromolecules* **1993**, *26*, 189.
(7) Dalvi, M. C.; Eastman, C. E.; Lodge, T. P. *Phys. Rev. Lett.* **1993**, *71*, 2591.
(8) Lodge, T. P.; Dalvi, M. C. *Phys. Rev. Lett.* **1995**, *75*, 657.
(9) Doi, M.; Edwards, S. F. *The Theory of Polymer Dynamics*; Oxford University Press: New York, 1986.
(10) Fredrickson, G. H.; Milner, S. T. *Mater. Res. Soc. Symp. Proc.* **1990**, *177*, 169.
(11) Barrat, J.-L.; Fredrickson, G. H. *Macromolecules* **1991**, *24*, 6378.
(12) Witten, T. A.; Leibler, L.; Pincus, P. A. *Macromolecules* **1990**, *23*, 824.
(13) Rubinstein, M.; Obukhov, S. P. *Macromolecules* **1993**, *26*, 1740.
(14) Fried, H.; Binder, K. *J. Chem. Phys.* **1991**, *94*, 8349.
(15) Weyersberg, A.; Vilgis, T. A. *Phys. Rev. E* **1993**, *48*, 377.
(16) Larson, R. G. *Macromolecules* **1994**, *27*, 4198.
(17) Molina, L. A.; Friere, J. J. *Macromolecules* **1995**, *28*, 2705.
(18) Haliloglu, T.; Balaji, R.; Mattice, W. L. *Macromolecules* **1994**, *27*, 1473.
(19) Ko, M. B.; Mattice, W. L. *Macromolecules* **1995**, *28*, 6871.
(20) Shaffer, J. S. *J. Chem. Phys.* **1994**, *101*, 4205.
(21) Shaffer, J. S. *J. Chem. Phys.* **1995**, *103*, 761.
(22) Carmesin, I.; Kremer, K. *Macromolecules* **1988**, *21*, 2819.
(23) Deutsch, H.-P.; Binder, K. *J. Chem. Phys.* **1991**, *94*, 2294.
(24) Allen, M. P.; Tildesley, D. J. *Computer Simulation of Liquids*; Oxford University Press: New York, 1987.
(25) Leibler, L. *Macromolecules* **1980**, *13*, 1602.
(26) Fredrickson, G. H.; Helfand, E. *J. Chem. Phys.* **1987**, *87*, 697.
(27) Matsen, M. W.; Bates, F. S. *Macromolecules* **1996**, *29*, 1091.
(28) Murat, M.; Grest, G. S. *Macromolecules* **1989**, *22*, 4054. From data in Table I of this reference, the ratio $r = 2\langle R^2_{g,\perp}\rangle/\langle R^2_{g,\parallel}\rangle$ can be as large as 18.5 for flexible off-lattice chains of length $N = 50$ at a grafting density of $\rho_a = 0.20$.
(29) Helfand, E. *Macromolecules* **1992**, *25*, 492.
(30) The diffusion coefficients for the homogeneous disordered phase (with $\chi = 0$) are those reported in ref 20, where no monomer−monomer energetics (other than athermal excluded volume interactions) were present.
(31) Kremer, K.; Grest, G. S. *J. Chem. Phys.* **1990**, *92*, 5057.
(32) Kavassalis, T. A.; Noolandi, J. *Phys. Rev. Lett.* **1987**, *59*, 2674.
(33) Colby, R. H.; Rubinstein, M.; Viovy, J. L. *Macromolecules* **1992**, *25*, 996.
(34) Fetters, L. J.; Lohse, D. J.; Richter, D.; Witten, T. A.; Zirkel, A. *Macromolecules* **1994**, *27*, 4639.
(35) Recent investigations of melt rheology reviewed in ref 34 suggest that the entanglement molecular weight is influenced by dynamical processes (not yet specifically identified) in addition to the structural features of polymer melts.

MA951907Y